

^{77}Se and ^{87}Rb Solid State NMR Study of the Structure of $\text{Rb}_2[\text{Pd}(\text{Se}_4)_2]\cdot\text{Se}_8$

A. Goldbach,[†] F. Fayon,[‡] T. Vosegaard,[§] M. Wachhold,^{||} M. G. Kanatzidis,^{||} D. Massiot,[‡] and M.-L. Saboungi^{*,†,⊥}

Institut für Grenzflächenverfahrenstechnik, Universität Stuttgart, Nobelstrasse 12, 70569 Stuttgart, Germany, Centre de Recherche sur les Matériaux à Haute Température (CRMHT), CNRS, 1D av. Recherche Scientifique, 45071 Orléans Cedex 2, France, Interdisciplinary Nanoscience Center (iNANO) and Laboratory for Biomolecular NMR Spectroscopy, Department of Molecular Biology, University of Aarhus, DK-8000 Aarhus C, Denmark, Department of Chemistry and Center for Fundamental Materials Research, Michigan State University, East Lansing, Michigan 48824, and Centre de Recherche sur la Matière Divisée, UMR 6619 CNRS–Université d'Orléans, 1bis rue de la Férollerie, 45071 Orléans Cedex 2, France

Received February 21, 2003

The structure of $\text{Rb}_2[\text{Pd}(\text{Se}_4)_2]\cdot\text{Se}_8$ has been investigated using ^{87}Rb magic angle spinning and static NMR and ^{77}Se magic angle spinning NMR. The number and the integrated intensities of the ^{87}Rb and ^{77}Se resonances are in full agreement with the crystallographic structure of the compound. The ^{87}Rb and ^{77}Se nuclear spin interaction parameters have been used to characterize the main structural units of the compound: infinite $[\text{Rb}(\text{Se}_8)]_x^{x+}$ columns and polymeric $[\text{Pd}(\text{Se}_4)_2]_x^{2x-}$ sheet anions.

Introduction

Recently, Wachhold and Kanatzidis discovered a layered ternary polyselenide, $\text{Rb}_2[\text{Pd}(\text{Se}_4)_2]\cdot\text{Se}_8$, that features an intriguing structural motif: sandwichlike coordinated $[\text{Rb}(\text{Se}_8)]_x^{x+}$ columns intersecting stacked layers of infinite polymeric $[\text{Pd}(\text{Se}_4)_2]_x^{2x-}$ sheet anions (Figure 1).¹ This finding came on the heels of reports that revealed new binary cesium tellurium compounds, $\text{Cs}_4\text{Te}_{28}^2$ and $\text{Cs}_3\text{Te}_{22}$,³ which hold homologous columnar $[\text{Cs}(\text{Te}_8)]_x^{x+}$ polycations and molecular $[\text{Cs}(\text{Te}_8)_2]^+$ clusters, respectively. Apparently, chalcogen rings form very stable coordination complexes with alkali metal ions in crystalline phases. Alkaline and alkaline earth ions may coordinate in a fashion similar to chalcogen species in disordered selenium/zeolite nanocom-

posites.^{4,5} Unfortunately, such coordination complexes cannot be easily detected within those materials employing conventional crystallographic techniques. On the other hand, high-resolution solid-state nuclear magnetic resonance (NMR) has proven to be a powerful tool for the investigation of structure and local bonding in solids such as polyselenides.^{6,7} Using this technique, valuable information can also be obtained from disordered materials, in particular, when conventional methods of structural analysis fail. In this paper, we report high-resolution solid-state ^{77}Se and ^{87}Rb NMR studies of the title compound, which can be viewed as a model compound for this novel class of sandwichlike chalcogenide–cation coordination complexes. In addition, we compare the solid-state ^{77}Se NMR spectrum of the polymeric $[\text{Pd}(\text{Se}_4)_2]_x^{2x-}$ sheet anions to solution ^{77}Se NMR data of a molecular $[\text{Pd}(\text{Se}_4)_2]^{2-}$ complex.^{8,9}

* To whom correspondence should be addressed. E-mail: MLS@cns-orleans.fr.

[†] Universität Stuttgart.

[‡] Centre de Recherche sur les Matériaux à Haute Température (CRMHT), CNRS.

[§] University of Aarhus.

^{||} Michigan State University.

[⊥] Centre de Recherche sur la Matière Divisée, UMR 6619 CNRS–Université d'Orléans.

(1) Wachhold, M.; Kanatzidis, M. G. *J. Am. Chem. Soc.* **1999**, *121*, 4189.

(2) Sheldrick, W. S.; Wachhold, M. *J. Chem. Soc., Chem. Commun.* **1996**, 607.

(3) Sheldrick, W. S.; Wachhold, M. *Angew. Chem., Int. Ed. Engl.* **1995**, *34*, 450.

(4) Goldbach, A.; Iton, L. E.; Saboungi, M.-L. *Chem. Phys. Lett.* **1997**, *281*, 69.

(5) Goldbach, A.; Saboungi, M.-L.; Iton, L. E.; Price, D. L. *J. Chem. Soc., Chem. Commun.* **1999**, 997.

(6) Barrie, P. J.; Clark, R. J. H.; Withnall, R.; Chung, D.-Y.; Kim, K.-W.; Kanatzidis, M. G. *Inorg. Chem.* **1994**, *33*, 1212.

(7) Barrie, P. J.; Clark, R. J. H.; Chung, D.-Y.; Chakrabarty, D.; Kanatzidis, M. G. *Inorg. Chem.* **1995**, *34*, 4299.

(8) Ansari, M. A.; Mahler, C. H.; Chorghade, G. S.; Lu, Y.-J.; Ibers, J. A. *Inorg. Chem.* **1990**, *29*, 3832.

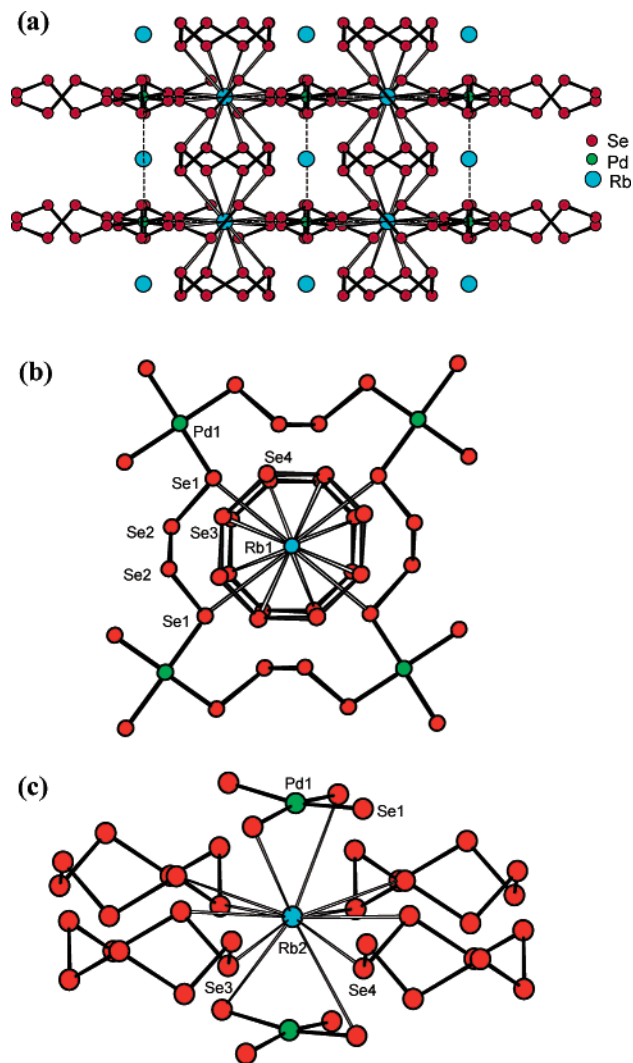


Figure 1. (a) Structure of $\text{Rb}_2[\text{Pd}(\text{Se}_4)_2] \cdot \text{Se}_8$ viewed along the [110] direction. (b, c) Coordination environment of the Rb(1) site (b) and the Rb(2) site (c) as determined by X-ray crystallography.¹

Experimental Section

The synthesis of $\text{Rb}_2[\text{Pd}(\text{Se}_4)_2] \cdot \text{Se}_8$ has been described in detail elsewhere.¹ In short, stoichiometric amounts of Rb_2CO_3 , PdCl_2 , $\text{Na}_2\text{-Se}$, and Se were mixed together in MeOH under dry atmosphere and then sealed in a Pyrex tube under vacuum. Then, the tube was heated for 48 h at 140 °C to yield quantitatively $\text{Rb}_2[\text{Pd}(\text{Se}_4)_2] \cdot \text{Se}_8$ as a black powder. Contingent impurity phases were not traceable by X-ray diffraction or solid-state NMR.

The ^{87}Rb NMR experiments were carried out on Bruker DSX400 (9.4 T) and DSX300 (7.0 T) spectrometers operating at ^{87}Rb Larmor frequencies of 130.9 and 98.2 MHz, respectively, using 4 mm MAS probeheads. In the case of quadrupolar nuclei affected by the second-order quadrupolar interaction, like ^{87}Rb (nuclear spin $I = 3/2$), the use of different principal fields allows variation of contrast between the second-order quadrupolar interaction (proportional to $1/B_0$) and the chemical shift anisotropy (proportional to B_0) in the experimental spectra, leading to an improved accuracy in the measurement of the two nuclear spin interactions. The ^{87}Rb static and magic angle spinning (MAS) NMR spectra were recorded using a Hahn echo sequence (rotor synchronized in the case of MAS

spectra) to obtain pure phase line shapes.¹⁰ The rf field strength was chosen to allow a selective excitation of the ^{87}Rb central transition ($\pi/2$ pulse duration of 1 μs). The recycle delay was set to 0.5 s. The ^{87}Rb chemical shifts were referenced relative to a 1.0 M RbNO_3 aqueous solution.

The ^{77}Se NMR experiments were carried out on the Bruker DSX400 (9.4T) spectrometer operating at the ^{77}Se (nuclear spin $I = 1/2$) Larmor frequency of 76.3 MHz, using 4 mm MAS probeheads. The ^{77}Se MAS NMR spectra were recorded using a single pulse acquisition with small pulse angle ($\pi/10$) and recycle delay of 5 s to ensure no saturation. The ^{77}Se chemical shifts were referenced relative to $\text{Se}(\text{CH}_3)_2$ at 0 ppm, using a saturated aqueous H_2SeO_3 solution as secondary reference ($\delta = 1282$ ppm vs $\text{Se}(\text{CH}_3)_2$).¹¹

All MAS spectra simulations were performed using the dmfit software¹² while the static ^{87}Rb spectra were simulated using SIMPSON¹³ in combination with the MINUIT¹⁴ minimization utilities.¹⁵ These simulations included effects from finite radio frequency pulses.

Results and Discussion

First, we briefly relate the structure of $\text{Rb}_2[\text{Pd}(\text{Se}_4)_2] \cdot \text{Se}_8$ as it was determined by X-ray crystallography in the initial study¹ of Wachhold and Kanatzidis since it is essential for the interpretation of the NMR spectra. A view of it down the [110] direction is displayed in Figure 1a. The analysis of the X-ray diffraction pattern yielded two different crystallographic sites for Rb and four for Se, but only one for Pd. The Pd atoms sit at the corners of 20-membered $\text{Pd}_4\text{Se}_{16}$ rings which constitute $[\text{Pd}(\text{Se}_4)_2]_x^{2x-}$ sheet anions as each Pd is coordinated by four Se_4^{2-} chains in a distorted square-planar environment as displayed in Figure 1b. The terminal and the center atoms of the Se_4^{2-} chains account for two of the crystallographically distinct Se sites, which were labeled Se(1) and Se(2), respectively. The other two sites were labeled Se(3) and Se(4) and belong to the crownlike Se_8 rings which are arranged in layers between the $[\text{Pd}(\text{Se}_4)_2]_x^{2x-}$ sheet anions. The Rb(1) atoms are located within the center of the $\text{Pd}_4\text{-Se}_{16}$ squares, and they are 4-fold coordinated in a sandwich-like fashion by each of two Se_8 rings above and below at distances of 3.851 and 3.870 Å (Figure 1a,b). This coordination scheme forms an infinite straight $[\text{Rb}(\text{Se}_8)]_x^{2x-}$ column running perpendicularly through layers of $[\text{Pd}(\text{Se}_4)_2]_x^{2x-}$ sheet anions (Figure 1a). Four additional, slightly longer contacts to Se(1) at 3.989 Å complete a coordination number of 12 for Rb(1) (Figure 1b). The Rb(2) atoms are located within the tetragonal plane of Se_8 rings and in a perpendicular direction directly between two Pd atoms with a short Rb(2)–Pd distance of 3.463 Å (Figure 1a,c). The Rb(2) atoms

(10) Massiot, D.; Farnan, I.; Gautier, N.; Trumeau, D.; Trokner, A.; Coutures, J. P. *Solid State Nucl. Magn. Reson.* **1995**, *4*, 241.

(11) Rodger, C.; Sheppard, N.; McFarlane, C.; McFarlane, W. *NMR and the Periodic Table*; Harris, R. K., Mann, B. E., Ed.; Academic Press: London, 1978; p 403.

(12) Massiot, D.; Fayon, F.; Capron, M.; King, I.; Le Calvé, S.; Alonso, B.; Durand, J. O.; Bujoli, B.; Gan, Z.; Hoatson, G. *Magn. Reson. Chem.* **2002**, *40*, 70.

(13) Bak, M.; Rasmussen, J. T.; Nielsen, N. C. *J. Magn. Reson.* **2000**, *147*, 296.

(14) James, F.; Ross, M. *Comput. Phys. Commun.* **1975**, *10*, 343.

(15) Vosegaard, T.; Malmendal, A.; Nielsen, N. C. *Monatsh. Chem.* **2002**, *133*, 1555.

(9) McConnachie, J. M.; Ansari, M. A.; Ibers, J. A. *Inorg. Chem.* **1993**, *32*, 3250.

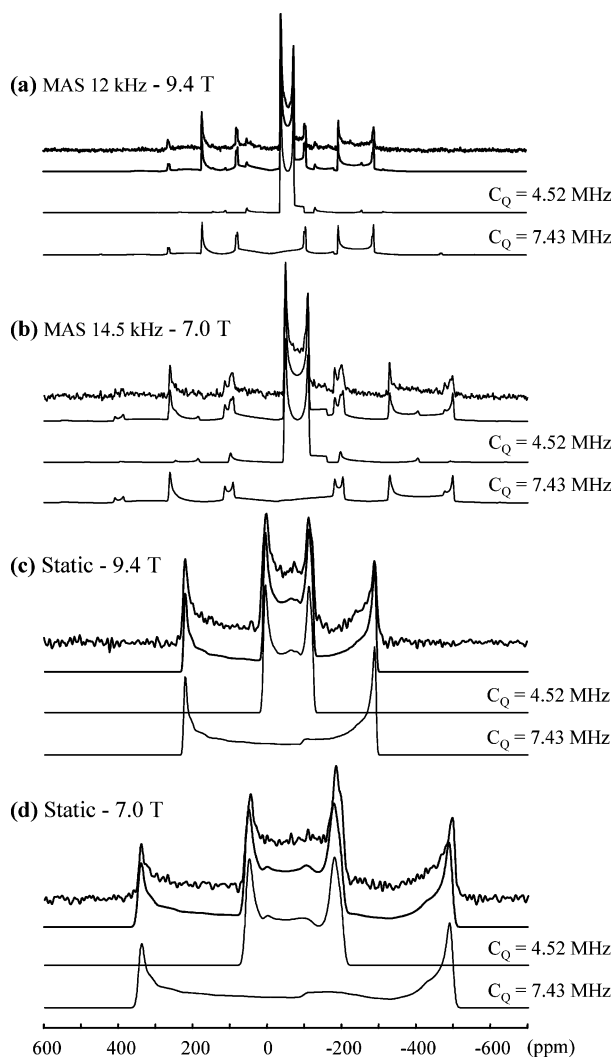


Figure 2. Experimental and simulated ^{87}Rb solid-state NMR spectra obtained at two different magnetic fields: (a) MAS spectrum at 9.4 T (12 kHz spinning rate), (b) MAS spectrum at 7.0 T (14.5 kHz spinning rate), (c) static spectrum at 9.4 T, and (d) static spectrum at 7.0 T.

are 12-fold Se-coordinated as well, to one Se(3) and one Se(4) atom, each of four surrounding Se_8 rings (distances of 4.085 and 4.095 Å, respectively), and to two opposing Se(1) sites each of the $[\text{Pd}(\text{Se}_4)_2]_{\text{X}}^{2-}$ sheet anions above and below (distance 4.044 Å).

Figure 2 shows the ^{87}Rb MAS and static NMR spectra recorded at two different magnetic fields (7.0 and 9.4 T). The MAS spectra exhibit well defined discontinuities that can be simulated by the $(-1/2, 1/2)$ central transitions of two ^{87}Rb resonances with overlapping spinning sidebands affected by the second order quadrupolar interaction. These two distinct resonances with second order quadrupolar line shapes are clearly resolved in the static spectra and show integrated intensities in the ratio 1:1, in good agreement with the multiplicities of the two crystallographic Rb sites of the structure. The chemical shift and quadrupolar parameters of the two ^{87}Rb resonances rendered by the simulation of the static and MAS spectra obtained at two different magnetic fields are reported in Table 1. The site assignment can be made on the basis of the ^{87}Rb quadrupolar coupling and chemical shift tensors, which are sensitive to the electronic

Table 1. Experimental Values from Solid-State ^{87}Rb NMR Experiments

site	δ_{iso}^a (ppm)	C_Q^b (MHz)	η_Q^b	δ_{csa}^a (ppm)	η_{csa}^a	β^c (deg)
Rb(1)	-29 ± 1	4.52 ± 0.02	0.07 ± 0.02	34 ± 5	0.00 ± 0.05	0
Rb(2)	18 ± 1	7.43 ± 0.02	0.00 ± 0.02	-115 ± 5	0.00 ± 0.05	0

^a $\delta_{\text{iso}} = (\delta_{\text{xx}} + \delta_{\text{yy}} + \delta_{\text{zz}})/3$, $\delta_{\text{csa}} = \delta_{\text{zz}} - \delta_{\text{iso}}$, and $\eta_{\text{csa}} = (\delta_{\text{yy}} - \delta_{\text{xx}})/\delta_{\text{csa}}$ with the principal components of the chemical shift tensor defined in the following sequence: $|\delta_{\text{zz}} - \delta_{\text{iso}}| \geq |\delta_{\text{xx}} - \delta_{\text{iso}}| \geq |\delta_{\text{yy}} - \delta_{\text{iso}}|$. ^b $C_Q = eQV_{\text{zz}}/h$ and $\eta_Q = (V_{\text{yy}} - V_{\text{xx}})/V_{\text{zz}}$ with the principal components of the electric field gradient tensor defined in the sequence $|V_{\text{zz}}| \geq |V_{\text{xx}}| \geq |V_{\text{yy}}|$. ^c β is defined as the angle between V_{zz} and δ_{zz} .

environment of the nucleus and its deviation from spherical symmetry. According to the crystal structure, the Rb atoms are located in special positions 2c (Rb(1)) and 2b (Rb(2)) with local 222 and $\bar{4}$ symmetries, respectively. The 4-fold rotation–inversion axis imposes axial symmetry of the nuclear spin interactions for Rb(2) while the 222 symmetry of Rb(1) implies that the principal elements of the quadrupole and chemical shift anisotropy (CSA) tensors must be aligned along these axes since the nuclear spin interactions must conform to the crystal symmetry.¹⁶ In addition, Rb(1) is coordinated to 12 Se while Rb(2) is coordinated to 2 Pd and 12 Se causing a significant difference in their local electronic environments. On the basis of these considerations, we may readily assign the Rb site with the larger quadrupole coupling constant and chemical shift anisotropy ($C_Q = 7.42$ MHz, $\delta_{\text{csa}} = -115$ ppm, $\delta_{\text{iso}} = 18$ ppm) to Rb(2) because of its axially distorted environment caused by the two Pd ions, which is expected to result in larger anisotropies of the nuclear spin interactions. This assignment is further supported by the fact that the quadrupole coupling and CSA tensors for this site show the expected axial symmetry ($\eta_Q = 0$, $\eta_{\text{csa}} = 0$). The remaining resonance with the smaller quadrupolar coupling constant and chemical shift anisotropy ($C_Q = 4.52$ MHz, $\delta_{\text{csa}} = 34$ ppm, $\delta_{\text{iso}} = -29$ ppm) is thus assigned to Rb(1) which is only coordinated to Se atoms. For the two Rb resonances, the principal axes of the electric field gradient and CSA tensors were found collinear from the simulations of the ^{87}Rb NMR spectra.

The ^{77}Se MAS NMR spectrum recorded at 9.4 T (10 kHz spinning rate) is reproduced in Figure 3. It clearly evidences four distinct isotropic resonances located at 652, 648, 627, and 551 ppm with integrated intensities in the ratio 1:1:1:1, corresponding to the four Se crystallographic sites in the structure. The ^{77}Se chemical shift anisotropy tensors of these four resonance peaks were determined from the spinning sideband intensities in the MAS spectrum¹⁷ and are reported in Table 2. Just one of the tabulated ^{77}Se resonances is clearly distinctive showing a significantly lower ^{77}Se isotropic chemical shift at 551 ppm. In the structure, Se(2), Se(3), and Se(4) are chemically bonded only to other Se atoms while Se(1) is also bonded to the Pd atom. Hence, we attribute the signal at 551 ppm to the Se(1) site. The other three isotropic chemical shifts are rather similar, and a straightforward Se site assignment is not possible. We have

(16) Cohen, M. H.; Reif, F. *Solid State Phys.* **1957**, *5*, 321.

(17) Herzfeld, J.; Berger, A. E. *J. Chem. Phys.* **1980**, *73*, 6021.

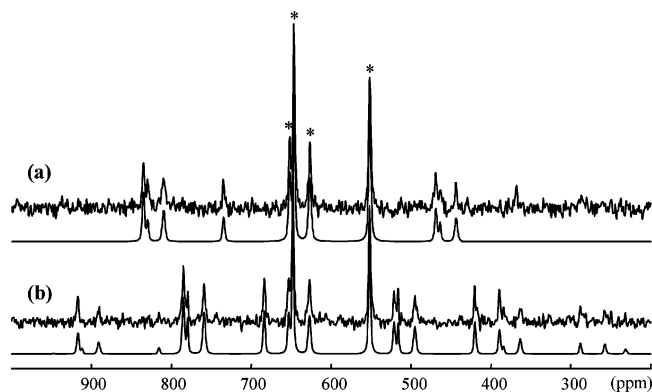


Figure 3. Experimental and simulated ^{77}Se MAS NMR spectra at (a) 14 and (b) 10 kHz spinning rate. The asterisks mark the isotropic lines.

Table 2. Experimental Values from Solid-State ^{77}Se NMR Experiments

	δ_{iso}^a (ppm)	δ_{csa}^a (ppm)	η_{csa}^a
site Se(1)	551 ± 1	-260 ± 10	0.65 ± 0.05
site Se(2)	648 ± 1	-210 ± 10	0.70 ± 0.05
sites Se(3), Se(4)	627 ± 1	-390 ± 10	0.70 ± 0.05
	652 ± 1	-450 ± 10	0.65 ± 0.05

$^a \delta_{\text{iso}} = (\delta_{xx} + \delta_{yy} + \delta_{zz})/3$, $\delta_{\text{csa}} = \delta_{zz} - \delta_{\text{iso}}$, and $\eta_{\text{csa}} = (\delta_{yy} - \delta_{xx})/\delta_{\text{csa}}$ with the principal components of the chemical shift tensor defined in the following sequence: $|\delta_{zz} - \delta_{\text{iso}}| \geq |\delta_{xx} - \delta_{\text{iso}}| \geq |\delta_{yy} - \delta_{\text{iso}}|$.

not been able to detect $J(\text{Se}-\text{Se})$ couplings that would assist with the assignment of resonances. The intensities of the satellites at natural abundance are low (^{77}Se ca. 7%), and the expected coupling magnitudes of 20–120 Hz as measured on ^{77}Se enriched samples¹⁸ are less than the line widths of the observed resonances (200 Hz). However, the two sites of the Se_8 ring are not expected to differ immensely in their ^{77}Se chemical shift parameters. Therefore, we assign the resonances at 627 and 652 ppm to Se(3) and Se(4) on account of the similar chemical shift tensors and, in particular, the similar chemical shift anisotropy, although an exact site assignment cannot be made. These two resonances are shifted slightly downfield with respect to the ^{77}Se NMR resonance at 614.6 ppm of neutral Se_8 molecules dissolved in CS_2 .¹⁹ The chemical shift variations can arise both from differing ring geometries in the $Rb_2[Pd(Se_4)_2] \cdot Se_8$ crystal and in CS_2 solution, and from differing coordination by the solvent CS_2 and the Rb^+ ions, respectively. The shifts attributed to Se_8 are in good agreement with general trends of isotropic ^{77}Se NMR shifts observed in different chemical bonding situations.^{8,20} The remaining ^{77}Se resonance at 648 ppm is attributed to the Se(2) site then. This assignment could be confirmed by through-bond correlation experiments using a ^{77}Se enriched sample.²¹

The assignment of the ^{77}Se resonances of the $[\text{Pd}(\text{Se}_4)_2]_x^{2x-}$ sheet anions requires careful consideration. The signals at 551 (terminal) and 648 ppm (central) attributed to the Se_4^{2-} chains differ clearly from those at 893 ppm (terminal Se_4^{2-}

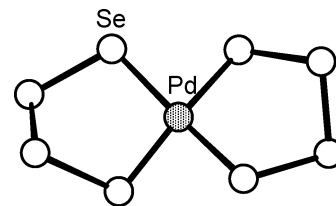


Figure 4. Molecular $[\text{Pd}(\text{Se}_4)_2]^{2-}$ rotor anion in $[\text{NET}_4]_5[2\text{Pd}(\text{Se}_4)_2 \cdot 0.5\text{Pd}(\text{Se}_5)_2]$.⁹

chain atom) and 758 ppm (central Se_4^{2-} chain atom) obtained in DMF solution for molecular $[\text{Pd}(\text{Se}_4)_2]^{2-}$ complexes, which nominally have the same stoichiometry.^{8,9} Note that the relative positions of the resonances of the terminal and the center Se atoms in the tetraselenide chain are also reversed when compared to those of the $[\text{Pd}(\text{Se}_4)_2]_x^{2x-}$ sheet anions. In $[\text{Ph}_4\text{P}]_2[\text{Pd}(\text{Se}_4)_2]^{8-}$ and $[\text{NET}_4]_5[2\text{Pd}(\text{Se}_4)_2 \cdot 0.5\text{Pd}(\text{Se}_5)_2]$,⁹ isolated rotorlike $[\text{Pd}(\text{Se}_4)_2]^{2-}$ units (Figure 4) exist since both ends of the Se_4^{2-} chains coordinate to the same Pd^{2+} ion. Thus, bond distances, bond angles, and torsion angles, in particular, differ from the rotor complex to the polymeric sheet anion. The large deviations between the respective ^{77}Se NMR resonances cannot be related in a simple fashion to differing structural parameters although the solid-state structure of $[\text{NET}_4]_5[2\text{Pd}(\text{Se}_4)_2 \cdot 0.5\text{Pd}(\text{Se}_5)_2]$ is known.⁹ The rotor anions adopt a conformation in the crystal which is likely to be different from its conformation in a DMF solvation cage. Thus, their structural parameters could differ notably from that of the distorted⁹ solid-state rotor anions. Furthermore, the terminal Se_4^{2-} chain atoms of the $[\text{Pd}(\text{Se}_4)_2]_x^{2x-}$ sheet anions coordinate to both Rb ions. This additional coordination will influence the ^{77}Se chemical shift as well.

However, the electronic interaction between the Pd^{2+} ions and the Se_4^{2-} chains has probably the strongest effect on Se NMR resonances. The uncomplexed tetraselenide carries formal charges of -1 at the terminal (t) and of 0 at the central (c) Se atoms. The t-Se atoms resonate upfield of the c-Se atoms in the case of Se_4^{2-} dissolved in DMF which shows resonances at $\delta_{\text{t-se}} = 301$ ppm and $\delta_{\text{c-se}} = 591$ ppm at 230 K.²⁰ The upfield shift of the t-Se resonance is even stronger when Se_4^{2-} is bound to the closed shell d^{10} -metal ion Cd^{2+} with $\delta_{\text{t-se}} = 62$ ppm and $\delta_{\text{c-se}} = 608$ ppm ($[\text{Cd}(\text{Se}_4)_2]^{2-}$ rotor complexes in DMF solution).⁸ The reversal of this situation for the corresponding $[\text{Pd}(\text{Se}_4)_2]^{2-}$ complexes has been linked to the d^8 open shell configuration of the Pd^{2+} ion, and it was argued that electron density is transferred from the tetraselenide ligands to the transition metal ions.⁸ This effect shifts the resonance of the central Se_4^{2-} chain atoms in the same direction, i.e., 758 ppm for $[\text{Pd}(\text{Se}_4)_2]^{2-}$ versus 608 ppm for $[\text{Cd}(\text{Se}_4)_2]^{2-}$.⁸ The assignment of the ^{77}Se resonance of the $[\text{Pd}(\text{Se}_4)_2]_x^{2x-}$ sheet anions is in agreement with these considerations (see Table 3). However, the resonances of the central and terminal Se atoms of the sheet anion are not reversed because electron transfer occurs to a smaller extent than in the case of the molecular ions. This is understood because electron exchange requires an overlap of the respective Se 4p and Pd 4d orbitals. The conformational flexibility of molecules is certainly larger than that of crystalline sheet anions, and a less than optimum configu-

(18) Laitinen, R. S.; Pakkanen, T. A. *Inorg. Chem.* **1987**, *26*, 2598.

(19) Laitinen, R. S.; Pakkanen, T. A. *J. Chem. Soc., Chem. Commun.* **1986**, 1381.

(20) Cusick, J.; Dance, I. *Polyhedron* **1991**, *10*, 2629.

(21) Fayon, F.; Le Saout, G.; Emsley, L.; Massiot, D. *J. Chem. Soc., Chem. Commun.* **2002**, 1702.

Table 3. ^{77}Se Isotropic Chemical Shifts of Tetraselenide Ions in Selected Metal Complexes

compd	$\delta_{\text{t-Se}}$ (ppm)	$\delta_{\text{c-Se}}$ (ppm)	ref
$[\text{Cd}(\text{Se}_4)_2]^{2-}$, in DMF	62	608	8
Se_4^{2-} , in DMF	301	591	20
$[\text{Pd}(\text{Se}_4)_2]^{2-}$	551	648	this work
$[\text{Pd}(\text{Se}_4)_2]^{2-}$, in DMF	893	758	8

ration of the sheet anions impedes the orbital overlap, which in return results in a weaker downfield shift of the Se NMR signals as observed. It could be argued that the Se resonances of the polymeric $[\text{Pd}(\text{Se}_4)_2]_x^{2x-}$ sheet anions are inverted as in the case of the molecular $[\text{Pd}(\text{Se}_4)_2]^{2-}$ rotor anions. However, this implies an improbable upfield shift of the c-Se resonance with respect to uncomplexed Se_4^{2-} while the t-Se signal would be strongly shifted in opposite directions at the same time. This has only been observed for polyselenide ligands bound in highly electron deficient d^0 and d^2 transition metal complexes so far.⁸ Hence, we consider the assignment of ^{77}Se resonances most plausible as given in Table 2. This attribution could possibly be corroborated by NMR spectroscopy if the Pt homologue of the title compound was available. ^{77}Se – ^{195}Pt coupling has been previously observed for $[\text{Pt}(\text{Se}_4)_2]^{2-}$ anions allowing an unequivocal identification of t- and c-Se atoms in these Pt bound tetraselenides.^{8,9}

Conclusion

High resolution ^{77}Se and ^{87}Rb solid-state MAS NMR spectra have been measured for the layered ternary polyse-

lenide, $\text{Rb}_2[\text{Pd}(\text{Se}_4)_2] \cdot \text{Se}_8$, which consists of infinite sandwichlike coordinated $[\text{Rb}(\text{Se}_8)]_x^{x+}$ columns intersecting layers of infinite $[\text{Pd}(\text{Se}_4)_2]_x^{2x-}$ sheet anions. The $[\text{Rb}(\text{Se}_8)]_x^{x+}$ columns are characterized by a ^{87}Rb resonance with an isotropic chemical shift of -29 ppm and two ^{77}Se NMR resonances with isotropic chemical shift values of 627 and 652 ppm. The second ^{87}Rb resonance with an isotropic chemical shift of 18 ppm is the signature of the Rb^+ ions located between the rings within the layers of Se_8 crowns. Two ^{77}Se NMR resonances with isotropic chemical shift values of 551 and 647 ppm are assigned to the metal bound and the central Se_4^{2-} chain atoms of the polymeric $[\text{Pd}(\text{Se}_4)_2]_x^{2x-}$ sheet anions. Both resonances are significantly upfield shifted in comparison to those of isostoichiometric molecular $[\text{Pd}(\text{Se}_4)_2]^{2-}$ anions. These shift variations are attributed to the general structural differences and the concomitant modification of the electronic interaction between the Pd^{2+} and the Se_4^{2-} ions.

Acknowledgment. F.F., T.V., and D.M. acknowledge financial support by European Community Contract HPRI-CT-1999-00042. T.V. acknowledges financial support from the Carlsberg foundation. M.W. and M.G.K. thank the National Science Foundation (Grant DMR-0127644) for financial support.

IC030074M